Title

Capture and characterization of influenza A virus from primary samples using glycan bead arrays.

Authors

Cohen, Miriam
Fisher, Christopher J
Huang, Mia L
et al.

Publication Date

2016-06-01

DOI

10.1016/j.virol.2016.03.011

Peer reviewed

Published in final edited form as:

Virology. 2016 June ; 493: 128–135. doi:10.1016/j.virol.2016.03.011.

Capture and characterization of influenza A virus from primary samples using glycan bead arrays

Miriam Cohen[a,*], **Christopher J. Fisher**[b], **Mia L. Huang**[b], **LeAnn L. Lindsay**[c], **Magdalena Plancarte**[c], **Walter M. Boyce**[c], **Kamil Godula**[b], and **Pascal Gagneux**[a,*]

[a]Department of Pathology, Division of Comparative Pathology and Medicine, UC San Diego, La Jolla, CA, USA

[b]Department of Chemistry and Biochemistry, UC San Diego, La Jolla, CA, USA

[c]Department of Pathology, Microbiology and Immunology, School of Veterinary Medicine, UC Davis, Davis, CA, USA

Abstract

Influenza A viruses (IAVs) utilize sialylated host glycans as ligands for binding and infection. The glycan-binding preference of IAV hemagglutinin (HA) is an important determinant of host specificity. Propagation of IAV in embryonated chicken eggs and cultured mammalian cells yields viruses with amino acid substitutions in the HA that can alter the binding specificity. Therefore, it is important to determine the binding specificity of IAV directly in primary samples since it reflects the actual tropism of virus in nature. We developed a novel platform for analysis of IAV binding specificity in samples that contain very low virus titers. This platform consists of a high-density flexible glycan display magnetic beads, which promotes multivalent interactions with the viral HA. Glycan-bound virus is detected by quantifying the viral neuraminidase activity via a fluorogenic reporter, 2'-(4–methylumbelliferyl)-α-D-*N*-acetylneuraminic acid. This method eliminates the need for labeling the virus and significantly enhances the sensitivity of detection.

Keywords

Influenza A; sialic acids; glycan array; magnetic beads; neuraminidase; glycans

Introduction

Influenza A viruses (IAVs) are extremely diverse and exist in the abundant and widespread reservoir of migratory aquatic birds (1). It is the combination of this natural reservoir with large and globally distributed populations of susceptible farm animals (ducks, chickens and pigs) that contributes to an omnipresent threat of new emerging zoonotic viruses and IAV

*Corresponding author: Miriam Cohen, Department of Pathology, UC San Diego. Phone: 858-717-6544, Fax: 858-534-5611, micohen@ucsd.edu.

*Pascal Gagneux, Department of Pathology, UC San Diego. Phone: 858-822-4030, Fax: 858-534-5611, pgagneux@ucsd.edu

pandemics. A recent example was the influenza (H1N1) pandemic of 2009 caused by a triple reassortment of bird, human and pig viruses (2). Aquatic birds are thus subject to surveillance for the early detection of newly emerging strains with enhanced potential to infect humans. The host specificity of IAV is determined to a large extent by the binding specificity of the virus hemagglutinin (HA) to host glycans (3, 4). The development of glycan arrays revolutionized analysis of IAV specificity for host glycans. Glycan arrays enable testing the binding specificity of purified HA and whole IAV to hundreds of glycans simultaneously (5, 6). Pioneering work by Stevens *et al* (7) revealed that human-specific IAVs bind to host sialic acids with α2-6 glycosidic linkage to the underlying glycan (α2-6Sia), while avian adapted IAVs overwhelmingly recognize α2-3 linked sialic acids (α2-3Sia). During the 2009 pandemic, glycan microarray studies revealed the wide binding specificity of the pandemic influenza A(H1N1) virus(8).

Typically, IAVs are isolated from host animals or environmental sources and propagated in embryonated chicken eggs ('eggs') or cultured mammalian cells ('cells') prior to assessing binding specificity on glycan microarrays (7, 9–11). It has been noted that the HA accumulates amino acids substitutions that affect the binding specificity to sialic acids (12, 13). IAV isolates that were grown in eggs acquire specificity for binding α2-3Sia, while the same isolates grown in cultured cells have broad specificity for both α2-3Sia and α2-6Sia (12). Therefore, analyzing the binding specificity of IAV directly from primary samples is highly valuable since it reflects the actual tropism of virus in nature.

The binding affinity of a single HA trimer to sialoglycans is low (14), requiring multivalent interactions to achieve high avidity binding. An average-sized, single IAV virion is estimated to have 500–1000 HA trimers, and 100–500 neuraminidase (NA) tetramers, on its envelope (15–17). The HA and NA are not evenly distributed on the virion, but instead are clustered, creating patches with high local densities (17). Host epithelial cells are covered with a dense matrix of glycoconjugates (glycocalyx) that can be anchored and/or secreted into the mucus layers. In vertebrates, most of these glycoconjugates carry multiple glycan chains, commonly terminating in sialic acid. Therefore, IAV likely engages multiple sialylated glycan chains on the host cell to achieve high avidity binding. Keeping this in mind, we developed a three-dimensional mucin mimetic array in which a large number of defined glycans are presented on a polymer backbone that extends from a magnetic bead core (Fig. 1). This unique high-density and flexible glycan display enhances multivalent binding by the virus, and reduces the viral titer required for reliable detection of binding (18).

Here we demonstrate the sensitivity and versatility of our novel three-dimensional mucin-mimetic array for characterizing various subtypes of avian IAV that were isolated from waterfowls. In addition, we provide a proof of principle for the analysis of IAV directly in primary samples. We analyzed swab samples collected from the cloaca of mallard ducks (*Anas platyrhynchos*) by applying them directly on the mucin mimetic beads. Thus, the array eliminates the need to amplify the virus prior to characterizing the receptor specificity, thereby limiting the risk of viral binding specificity changes due to amino acid substitutions in the HA.

Results and Discussion

Low virus concentrations suffice for analysis on the 3D mucin mimetic array

Multivalent interactions between viral HA and the sialylated polymers are likely affected by the spacing between sialylated polymers on the beads, and both glycan density and the concentration of IAV are known to affect virus binding to glycan microarrays (10). In order to determine the optimal density for IAV binding, the mucin mimetic polymers were conjugated to magnetic beads at densities ranging between 1–50 polymers/1600 nm^2 (Supplementary Fig. 1). The binding of A/PR/8/34(H1N1) was tested at virus concentrations of 9.2–160 HAU/ml (Fig. 2a–b and supplementary Fig. 2). The bound virus was detected by incubation with the reporter molecule, 2'-(4–Methylumbelliferyl)-α-D-*N*-acetylneuraminic acid (4MU-NANA, 4MUNeu5Ac). The viral NA cleaves sialic acid from the 4MU-Neu5Ac compounds thereby releasing a fluorescent 4-methylumbelliferone molecule (4MU). Release of 4MU (pmol/1h) is indicative of viral activity and correlates with viral titers (19). In order to minimize interference from NA cleaving of the glycosylated beads, 6 mmol of the 4MU-Neu5Ac compounds were added to the beads. This method is highly sensitive and enables detection of IAV at concentrations as low as 5 HAU/ml (Fig. 2c). In comparison, IAV binding to the Consortium for Functional Glycomics glycan array typically requires 2,500–10,000 HAU/ml IAV(10, 20, 21). Virus binding to the bead array was detected when the density of polymer was larger or equal to ~12 polymers/1600 nm^2 (Fig. 2a–b). Interestingly, Harris *et al.* reported an average of 13 HA trimers in 1600 nm^2 of viral envelope (17). Beads covered with high-density polymers enabled detection of A/PR/8/34(H1N1) at concentrations as low as 9.2 HAU/ml (orange circle, Fig.2a–b) nearly the detection limit obtained with the 4MU-NANA assay (5 HAU/ml, Fig. 2c). The same mucin mimetic polymer printed on microarray slides requires at least 25 fold more concentrated A/PR/8/34(H1N1) virus for reliable detection (18) (Supplementary Fig. 3).

Validation of the 3D mucin mimetic array

We generated a library of 43 mucin mimetic polymers conjugated to magnetic beads by incubating streptavidin-conjugated magnetic beads with 43 biotinylated mucin mimetic polymers (Fig. 3). The ligand library comprises 19 sialylated glycoconjugates (Fig. 3 **1–19**), and their corresponding non-sialylated backbone (Fig. 3 **22–23, 29–32**). In addition the library contains the ABO blood group antigens (Fig. 3 **20,24–25**) and Lewis blood group glycans (Fig. 3 **16–17, 22–23, 26–27**), which are typically found in the mucus and mucosa layers, sialylated gangliosides (Fig. 3 **9, 13–15**) and monosaccharides (Fig. 3 **28, 34–43**). The mucin mimetic beads were analyzed by flow cytometry and the polymers density on the beads was calculated for each glycan structure. The average density was 28 glycopolymers/1600 nm^2 (Supplementary Tables 1–2 and Supplementary Fig. 4a). Two human IAV strains A/PR/8/34(H1N1) and A/Aichi/2/68(H3N2) were diluted in PBS to 64 HAU/ml, and their binding to the array was tested (Fig. 4a–b). Since virus bound to the array is quantified by measuring NA activity, we confirmed that the NA activity of both strains is comparable (Fig. 4c). In agreement with previous reports, both strains bound exclusively to glycoconjugates with terminal sialic acids in both α2-3- and α2-6- linkage to the underlying glycans (22–26). Conventional glycan array studies (27) have shown that A/PR/8/34(H1N1) has a preference for binding sialic acids in terminal position (Fig. 4a, **glycans 1–10**) but not internally linked

sialic acids (Fig. 4a, **glycans 14–15**), and for binding sialyl Lewis A but not sialyl Lewis X (Fig. 4a, **glycans 16–17**). Binding of A/Aichi/2/68(H3N2) to α2-3- and α2-6-sialylated glycans (Fig. 4b, **glycans 1–10**) was previously demonstrated by biolayer interferometry receptor binding assay, and agglutination assay (26). The binding preference to GM1b (Fig. 4b **glycan 9**) but not GM1a or fucosyl GM1a (Fig. 4b **glycans 14, 19**) was previously demonstrated by agglutination of gangliosides infused into asialo- erythrocytes (24). Interestingly, despite having the same NA activity, a higher signal was obtained for A/PR/8/34(H1N1) strain compared with A/Aichi/2/68(H3N2) strain. This may indicate lower binding affinity of the H3N2 strain to the glycoconjugates.

Binding of avian IAV to the array

There is an ongoing effort to identify and monitor changes in the binding specificity of potential zoonotic and pandemic IAVs. Of particular interest are IAV strains that acquire binding specificity to the α2-6Sia. Swab samples are routinely collected from aquatic birds and marine mammals for detection and subsequent isolation of circulating IAV strains (1, 28). On the bead array, bound virus is detected by quantifying NA activity of the bead-bound virions. There is no need to infuse the virions with fluorescent dye or to generate strain-specific antibodies. Therefore, the bead array is useful for investigating IAV from all subtypes, provided that the virions have active NA. To confirm this, six subtypes of low pathogenicity avian IAV were isolated from cloacal and environmental swabs of waterfowl, propagated in eggs, and tested on a subset of the array (Fig. 5a–f). This subset comprised paired glycoconjugates differing only with regard to their terminal sialic acids (linked in either α2-3 or α2-6 glycosidic linkage), and included also non-sialylated glycoconjugates as controls (Supplementary Table 3 and Supplementary Fig. 4b). Since detection of virus binding to the bead array is based on NA activity, the activity for each viral strain was independently tested (Fig. 5, activity is noted on the graphs). Note the low NA activity (6–41 pmol/1h) in four of the viruses tested (Fig. 5 a–c and e), which is lower than the NA activity of 9.6 HAU/ml A/PR/8/34(H1N1) depicted in Fig 2c. Specific binding to α2-3Sia was detected for A/mallard/California/2762/2012(H3N8), A/northern pintail/California/3466/2010(H1N3), A/environmental/California/7451/2010(H7N3) and A/mallard/California/1438/2010(H2N3) (Fig 5a–d); A binding pattern that is typical for many low pathogenicity avian IAV strains.

Interestingly, two of the strains A/mallard/California/1490/2013(H5N5) and A/mallard/California/14-320/2014(H2N1) bound to α2-6Sia in addition to the α2-3Sia glycoconjugates (Fig 5e–f). Despite exposing the array to high NA activity stock of H5N5 strain, the signal from bead-bound virus was low. This suggests that the binding of A/mallard/California/1490/2013(H5N5) strain to host glycans is of low affinity but broad specificity. To further validate these findings we used the Sequence Derived Phenotype Marker tool at the Influenza Research Database website (http://www.fludb.org/brc/home.spg?decorator=influenza) to analyze the HA sequence for IAV strain A/mallard/California/1490/2013(H5N5). A number of mutations in the HA segment that are known to enhance α2-6 binding without affecting α2-3 binding were identified including 110N, 171N, 172A, 226I, and 251P (29–31). Thus, this tool, which is only available for H5 subtypes, verified that the binding to the 3D mucin mimetic array was in agreement with the predictions based

on sequence analysis. In addition, the human IAV strains, A/PR/8/34(H1N1) and A/Aichi/2/68(H3N2) were also tested on the subset array (Fig. 5g–h). The human IAV strains bound to sialylated glycopolymers, as expected. These results confirm that IAV with low NA activity (6–40 pmol 4MU /1h) can be analyzed on the 3D mucin mimetic array.

Analysis of IAV in swab samples

The enzymatic detection of bead-bound virus enabled analysis of IAV at low titers and without prior labeling or manipulation. Therefore primary samples can be directly applied to the 3D mucin mimetic bead array. Five PCR-positive and two PCR-negative swab samples collected from the cloaca of mallard ducks (32) were analyzed on 3’ sialyllactose and 6’ sialyllactose mucin mimetic beads (Fig. 6). All five samples that tested positive for IAV by PCR bound the 3’ sialyllactose beads (Fig. 6a, black bars), two of these samples (2923V and 2540V) bound to 6’ sialyllactose as well (Fig. 6a, gray bars). Samples that were negative for IAV by matrix RTPCR (742CL and 743CL) did not bind to the beads. In addition, NA activity in each primary sample was independently quantified prior to incubation with the mimetic beads (Fig. 6c). Despite the high NA activity observed in one of the negative samples (743CL), which could presumably be attributed to bacterial NA or other contaminants, it did not produce false positive signal after bead purification.

We were intrigued by the fact that two of the samples (2923V and 2540V) exhibit binding to the 6’-sialyllactose beads, which may indicate potential ability to infect humans. To confirm these finding, we repeated the experiment using a different approach for detecting bead-bound virus. Following incubation of the samples with the beads, viral RNA was extracted from the bead-bound virus and quantified by RT-PCR (Fig. 6b). The primary samples that contained active virus were found on the 3’-sialyllactose beads, three of the samples were also found on the 6’sialyllactose beads (2923V, 2540V and 1367V). No measurable RNA was found on the lactose beads or with the negative primary sample 742CL. Due to the threshold cycle number (Ct) counts in the samples (Fig. 6b, $37<Ct<41$) subtyping of the bead bound virus was not possible (32).

Conclusion

The high density and spatial presentation of glycans on the 3D mucin mimetic beads strongly promotes multivalent interactions with the virions. In addition, bead bound virions are detected by quantifying the enzymatic activity of viral NA. This simultaneously enhances the signal and removes the need to label the virions for detection. As a result low abundance virus can be readily analyzed on the bead array, enabling analysis of IAV binding specificity directly from primary samples, while avoiding the inherent problem of amino acids substitutions that potentially occur during virus propagation in eggs or cultured cells. Furthermore, bead-bound virus can be detected by PCR, indicating that the array can be easily adapted for study of other glycan-binding viruses and bacteriophages.

The specificity of avian IAV to sialylated glycans is not an absolute but rather forms a continuum that constantly evolves (4). Avian IAV have the potential to bind sialic acids in both α2-3 and α2-6 glycosidic linkages to underlying structure, and deep sequencing analysis revealed that subpopulations of viruses are present in viral isolates (33). However,

in addition to the binding specificity, other viral factors (NS, polymers, NA) and host factors (adaptive and innate immune responses) are also critically important for pathogenesis (4). Our mucin mimetic bead array enables detection of binding phenotype directly in primary samples. Coupling the phenotypic data with full genome sequencing of IAV will help reveal genetic markers for IAV binding specificity.

Materials and Methods

Viruses and cultured cells

Madin-Darby Canine Kidney (MDCK) cells (ATCC CCL-34) were cultured in Dulbeco's modified Eagle's medium (DMEM, Cellgro) supplemented with 10% fetal calf serum (FCS), 100 U/ml penicillin, 100 U/ml streptomycin. Influenza virus strains A/PR/8/34 (H1N1) (ATCC VR-1469) and A/Aichi/2/68(H3N2) (ATCC 547) were purchased from ATCC and propagated in MDCK cells that were transferred to DMEM medium supplemented with 0.2% BSA fraction V (EMD), 25mM HEPES buffer (Gibco), 2 μg/ml TPCK-trypsin (Worthington Corporation), and 1% penicillin/streptomycin ("DMEM-TPCK" media). In addition, we analyzed six avian viruses that were isolated by egg inoculation from cloacal or environmental swabs as described by Lindsay *et al* (32). These strains and their Genbank accession numbers included: A/northern pintail/California/3466/2010(H1N3) CY120659-CY120666, A/mallard/California/1438/2010(H2N3) CY120563-CY120570, A/environmental/California/7451/2010(H7N3) CY120539-CY120146, A/mallard/California/2762/2012(H3N8) CY157086-CY157093, A/mallard/California/1490/2013(H5N5) CY177385–CY17792, A/mallard/California/14-320/2014(H2N1) KU160797

Virus titers were determined by hemagglutination test using 1% guinea pig erythrocytes (Lonza) for human IAV and 0.5% turkey erythrocytes (Lampire Biological Laboratories) for avian IAV and primary samples. The 50% tissue culture infective dose ($TCID_{50}$) was assayed in MDCK cells and calculated using the Spearman-Karber method (34). $TCID_{50}$ of A/PR/8/34(H1N1) at concentrations of 31.6–160 HAU/ml is $10^{4.5}$ and at concentrations of 9.1–21.2 HAU/ml is $10^{3.5}$.

3D-mucin mimetic beads preparation

Sera-Mag SpeedBeads Blocked Streptavidin (Thermo-Fisher cat# 2115-2104-011150, 1 μm diameter) were washed three times and resuspended in 125 mM PBS pH 7.4 (Gibco). Biotinylated mucin mimetic polymers were added at final concentration of 20–300 nM, and incubate 45 min at room temperature with rotation. The polymers-conjugated beads were washed with PBS pH 7.2 (Gibco) three times, and resuspended in PBS pH 7.2 supplemented with 0.02% sodium azide. Polymer conjugation to the beads was quantified by flow cytometry (BD FACSCaliber, BD-Biosciences). Sialic acid content of 6'sialyllactose, 3'sialyllactose and lactose beads was determined by 1,2-diamino-4,5-methylenedioxybenzene dihydrochloride–high performance liquid chromatography analysis (DMB-HPLC) according to a published protocol (35). Samples were incubated for 1h with 0.1M HCl at 80°C to release Sias, and filtered through microcon-3kDa filtration device (Millipore). Free Sialic acids were incubated for 2.5 h at 50°C in the dark with 7 mM DMB

(Sigma), 0.75 M 2-mercapto-ethanol, 18 mM Na-hydrosulfite in 1.4 M acetic acid. Sialic acids were separated on 250x4.6 mm Gemini C18 reverse phase column (Phenomenex) with 7% MeOH, 8% Acetonitrile, 85% H_2O solution at 0.9 ml/min using the ELITE Lachrom HPLC system (Hitachi). DMB-labeled Sialic acids were detected at EX=373 EM=488.

Detection of NA activity

The NA activity of IAV samples was determined by incubating 10 μl of the sample with 6 nmol 2'-(4–methylumbelliferyl)-α-D-N-acetylneuraminic acid (4MU-Neu5Ac) (Sigma-Aldrich) as previously described (19). Briefly, 40 μl of 0.15 mM 4MU-Neu5Ac in 33 mM 2-(N-Morpholino) ethanesulphonic acid (MES, Sigma-Aldrich), 120 mM NaCl2, 4 mM CaCl2 buffer pH 6.5 (MES/CaCl2/NaCl2 buffer) was added to the virus and incubated for 1 h at 37°C in dark. Following incubation 150 μl of 25% ethanol, 0.1M glycine pH 10.7 was added. The amount of released 4MU compound was measured at excitation 365 nm and emission 450 nm in a SpectraMax M3 spectrophotometer (Molecular Devices). To control for spontaneous degradation of the 4MU-Neu5Ac compound 50 μl 0.1mM 4MU-Neu5Ac signal was subtracted from all of the samples.

Virus binding to 3D mucin mimetic array

The mucin mimetic bead library was transferred to PCR plates (twin.tec PCR plates LoBind, Eppendorf). Each glycan structure was placed at 1.4×10^6 beads/well in three wells, washed three times with 100 μl PBS and resuspended in 50 μl PBS. All washes were done on a DynaMag-96 side skirted magnetic beads separator plate (Life Technologies), the PCR plate was shifted back and forth from left to right 10 times to mix the beads. IAV (50 μl) was added to the beads and the plate was sealed with microseal 'F' foil (Biorad). The plate was vortex-mixed and incubated at 4°C for 2h on a rocking shaker. Incubation was done at 4°C in order to inhibit enzymatic NA activity, however similar results were obtained by 1h incubation at 37°C. The beads were washed three times with PBS to remove unbound virus. Bead-bound virus was quantified by measuring viral NA activity, as described above with minor changes. The beads were resuspended in 60 μl of 0.1mM 4MU-Neu5Ac in 33 mM MES/$CaCl_2$/$NaCl_2$ buffer, and incubated for 1 h at 37°C in dark. Following incubation, 50 μl of the supernatant was transferred to 96-well plate, and 150 μl of 25% ethanol, 0.1M glycine pH 10.7 was added. Signal from 50 μl 0.1mM 4MU-Neu5Ac was subtracted from all of the samples. The amount of released 4MU compound was measured at excitation 365 nm and emission 450 nm in a SpectraMax M3 spectrophotometer.

Primary samples analysis on mucin mimetic beads

Wild mallard ducks (n = 7) were captured, cloacal swabs were collected and placed in separate vials containing 2 mL of ice-cold virus transport medium (VTM: Medium 199 with Earle's salts, L-glutamine, and sodium bicarbonate, plus 2 mU/L penicillin G, 200 mg/L streptomycin, 2 mU/L polymyxin B, 250 mg/L gentamicin, 0.5 mU/L nystatin, 60 mg/L ofloxacin, 200 mg/L sulfamethoxazole, and 0.5% bovine serum albumin V) (32). The samples were transported on ice to the laboratory where they were stored at −80 °C. The samples were subtyped at J. Craig Venter Institute as previously described (32). Before analysis on the mucin mimetic beads, the samples were thawed and centrifuged at 16,000g for 2 min to remove large precipitants. Mucin mimetic beads were placed in 96-well PCR

plate at 2.5 $\times 10^6$ beads/well, and washed three times with PBS. Twenty-five microliters of the supernatant were directly applied to the beads in triplicates, and incubated for 4°C for 2h. The beads were washed three times with PBS. For virus detection by NA activity the beads were resuspended in 60 μl of 0.1mM 4MU-Neu5Ac and NA activity was quantified as described above. Non-specific binding was corrected by subtracting Signal from lactose conjugated mucin mimetic bead wells. For virus detection by PCR the beads were resuspended in 50 μl DMEM-TPCK media. Viral RNA was extracted by adding 50 μl lysis buffer (without carrier RNA) from a MagMax-96 AI/ND Viral RNA isolation kit (Ambion Inc. Austin, TX, USA). A Kingfisher nucleic acid extraction system (Thermo Scientific) was used to extract RNA according to the MagMAX kit instructions. Complementary DNA was generated from 4 μL of RNA using a MMLV reverse transcriptase kit (Invitrogen, Carlsbad, CA, USA) following the manufacturer's protocol and using random primers. PCR was performed as previously described (32). Results from real-time PCR are reported in threshold cycle (Ct) values, which correspond to the number of PCR cycles required to detect nucleic acid (lower Ct numbers indicate greater concentration of virus RNA in the sample). Any sample with a Ct value ≥45, *i.e.*, exceeding the maximum number of cycles specified by the real-time PCR program, was considered negative (beyond detectable limits). An Applied Biosystems 7500 Fast instrument was used. All samples were tested twice, each time starting with the extracted RNA.

Supplementary Material

Refer to Web version on PubMed Central for supplementary material.

Acknowledgments

We thank Hadeel Hedo (UCSD) for excellent technical support. This study was supported in part by funding from NIH: CEIRS - HHSN272201400008C and HHSN266200700010C (WMB), NIH: NIBIB - 5 R00 EB013446-05 (KG), and by the G. Harold and Leila Y. Mathers Foundation of Mount Kisco, New York (PG). CF was supported in part by the UCSD Graduate Training Program in Molecular Biophysics through an institutional training grant from the National Institute of General Medical Sciences, T32 GM08326

References

1. Webster RG, Bean WJ, Gorman OT, Chambers TM, Kawaoka Y. Evolution and ecology of influenza A viruses. Microbiol Rev. 1992; 56:152–179. [PubMed: 1579108]
2. Garten RJ, Davis CT, Russell CA, Shu B, Lindstrom S, Balish A, Sessions WM, Xu X, Skepner E, Deyde V, Okomo-Adhiambo M, Gubareva L, Barnes J, Smith CB, Emery SL, Hillman MJ, Rivailler P, Smagala J, de Graaf M, Burke DF, Fouchier RA, Pappas C, Alpuche-Aranda CM, Lopez-Gatell H, Olivera H, Lopez I, Myers CA, Faix D, Blair PJ, Yu C, Keene KM, Dotson PDJ, Boxrud D, Sambol AR, Abid SH, St George K, Bannerman T, Moore AL, Stringer DJ, Blevins P, Demmler-Harrison GJ, Ginsberg M, Kriner P, Waterman S, Smole S, Guevara HF, Belongia EA, Clark PA, Beatrice ST, Donis R, Katz J, Finelli L, Bridges CB, Shaw M, Jernigan DB, Uyeki TM, Smith DJ, Klimov AI, Cox NJ. Antigenic and genetic characteristics of swine-origin 2009 A(H1N1) influenza viruses circulating in humans. Science. 2009; 325:197–201. [PubMed: 19465683]
3. Shi Y, Wu Y, Zhang W, Qi J, Gao GF. Enabling the 'host jump': structural determinants of receptor-binding specificity in influenza A viruses. Nat Rev Microbiol. 2014; 12:822–831. [PubMed: 25383601]
4. de Graaf M, Fouchier RA. Role of receptor binding specificity in influenza A virus transmission and pathogenesis. EMBO J. 2014; 33:823–841. [PubMed: 24668228]

5. Arthur CM, Cummings RD, Stowell SR. Using glycan microarrays to understand immunity. Curr Opin Chem Biol. 2014; 18:55–61. [PubMed: 24486647]
6. Smith DF, Cummings RD. Investigating virus-glycan interactions using glycan microarrays. Curr Opin Virol. 2014; 7:79–87. [PubMed: 24995558]
7. Stevens J, Blixt O, Glaser L, Taubenberger JK, Palese P, Paulson JC, Wilson IA. Glycan microarray analysis of the hemagglutinins from modern and pandemic influenza viruses reveals different receptor specificities. J Mol Biol. 2006; 355:1143–1155. [PubMed: 16343533]
8. Childs RA, Palma AS, Wharton S, Matrosovich T, Liu Y, Chai W, Campanero-Rhodes MA, Zhang Y, Eickmann M, Kiso M, Hay A, Matrosovich M, Feizi T. Receptor-binding specificity of pandemic influenza A (H1N1) 2009 virus determined by carbohydrate microarray. Nat Biotechnol. 2009; 27:797–799. [PubMed: 19741625]
9. Eisfeld AJ, Neumann G, Kawaoka Y. Influenza A virus isolation, culture and identification. Nat Protoc. 2014; 9:2663–2681. [PubMed: 25321410]
10. Gulati S, Lasanajak Y, Smith DF, Cummings RD, Air GM. Glycan array analysis of influenza H1N1 binding and release. Cancer Biomark. 2014; 14:43–53. [PubMed: 24643041]
11. Heimburg-Molinaro J, Tappert M, Song X, Lasanajak Y, Air G, Smith DF, Cummings RD. Probing virus-glycan interactions using glycan microarrays. Methods Mol Biol. 2012; 808:251–267. [PubMed: 22057531]
12. Stevens J, Chen LM, Carney PJ, Garten R, Foust A, Le J, Pokorny BA, Manojkumar R, Silverman J, Devis R, Rhea K, Xu X, Bucher DJ, Paulson JC, Cox NJ, Klimov A, Donis RO. Receptor specificity of influenza A H3N2 viruses isolated in mammalian cells and embryonated chicken eggs. J Virol. 2010; 84:8287–8299. [PubMed: 20519409]
13. Lee HK, Tang JW, Kong DH, Loh TP, Chiang DK, Lam TT, Koay ES. Comparison of mutation patterns in full-genome A/H3N2 influenza sequences obtained directly from clinical samples and the same samples after a single MDCK passage. PLoS One. 2013; 8:e79252. [PubMed: 24223916]
14. Sauter NK, Bednarski MD, Wurzburg BA, Hanson JE, Whitesides GM, Skehel JJ, Wiley DC. Hemagglutinins from two influenza virus variants bind to sialic acid derivatives with millimolar dissociation constants: a 500-MHz proton nuclear magnetic resonance study. Biochemistry. 1989; 28:8388–8396. [PubMed: 2605190]
15. Taylor HP, Armstrong SJ, Dimmock NJ. Quantitative relationships between an influenza virus and neutralizing antibody. Virology. 1987; 159:288–298. [PubMed: 3617501]
16. Markovic I, Leikina E, Zhukovsky M, Zimmerberg J, Chernomordik LV. Synchronized activation and refolding of influenza hemagglutinin in multimeric fusion machines. J Cell Biol. 2001; 155:833–844. [PubMed: 11724823]
17. Harris A, Cardone G, Winkler DC, Heymann JB, Brecher M, White JM, Steven AC. Influenza virus pleiomorphy characterized by cryoelectron tomography. Proc Natl Acad Sci U S A. 2006; 103:19123–19127. [PubMed: 17146053]
18. Huang ML, Cohen M, Fisher CJ, Schooley RT, Gagneux P, Godula K. Determination of receptor specificities for whole influenza viruses using multivalent glycan arrays. Chem Commun (Camb). 2015; 51:5326–5329. [PubMed: 25574528]
19. Nayak DP, Reichl U. Neuraminidase activity assays for monitoring MDCK cell culture derived influenza virus. J Virol Methods. 2004; 122:9–15. [PubMed: 15488615]
20. Lugovtsev VY, Smith DF, Weir JP. Changes of the receptor-binding properties of influenza B virus B/Victoria/504/2000 during adaptation in chicken eggs. Virology. 2009; 394:218–226. [PubMed: 19766280]
21. Chen LM, Rivailler P, Hossain J, Carney P, Balish A, Perry I, Davis CT, Garten R, Shu B, Xu X, Klimov A, Paulson JC, Cox NJ, Swenson S, Stevens J, Vincent A, Gramer M, Donis RO. Receptor specificity of subtype H1 influenza A viruses isolated from swine and humans in the United States. Virology. 2011; 412:401–410. [PubMed: 21333316]
22. Rogers GN, Paulson JC. Receptor determinants of human and animal influenza virus isolates: differences in receptor specificity of the H3 hemagglutinin based on species of origin. Virology. 1983; 127:361–373. [PubMed: 6868370]

23. Cohen M, Zhang XQ, Senaati HP, Chen HW, Varki NM, Schooley RT, Gagneux P. Influenza A penetrates host mucus by cleaving sialic acids with neuraminidase. Virol J. 2013; 10:321. [PubMed: 24261589]
24. Suzuki Y, Matsunaga M, Nagao Y, Taki T, Hirabayashi Y, Matsumoto M. Ganglioside GM1b as an influenza virus receptor. Vaccine. 1985; 3:201–203. [PubMed: 4060848]
25. Matrosovich MN, Gambaryan AS, Tuzikov AB, Byramova NE, Mochalova LV, Golbraikh AA, Shenderovich MD, Finne J, Bovin NV. Probing of the receptor-binding sites of the H1 and H3 influenza A and influenza B virus hemagglutinins by synthetic and natural sialosides. Virology. 1993; 196:111–121. [PubMed: 8356788]
26. Lin YP, Xiong X, Wharton SA, Martin SR, Coombs PJ, Vachieri SG, Christodoulou E, Walker PA, Liu J, Skehel JJ, Gamblin SJ, Hay AJ, Daniels RS, McCauley JW. Evolution of the receptor binding properties of the influenza A(H3N2) hemagglutinin. Proc Natl Acad Sci U S A. 2012; 109:21474–21479. [PubMed: 23236176]
27. Blixt O, Head S, Mondala T, Scanlan C, Huflejt ME, Alvarez R, Bryan MC, Fazio F, Calarese D, Stevens J, Razi N, Stevens DJ, Skehel JJ, van Die I, Burton DR, Wilson IA, Cummings R, Bovin N, Wong CH, Paulson JC. Printed covalent glycan array for ligand profiling of diverse glycan binding proteins. Proc Natl Acad Sci U S A. 2004; 101:17033–17038. [PubMed: 15563589]
28. Webster RG, Govorkova EA. Continuing challenges in influenza. Ann N Y Acad Sci. 2014; 1323:115–139. [PubMed: 24891213]
29. Watanabe Y, Ibrahim MS, Ellakany HF, Kawashita N, Mizuike R, Hiramatsu H, Sriwilaijaroen N, Takagi T, Suzuki Y, Ikuta K. Acquisition of human-type receptor binding specificity by new H5N1 influenza virus sublineages during their emergence in birds in Egypt. PLoS Pathog. 2011; 7:e1002068. [PubMed: 21637809]
30. Wang W, Lu B, Zhou H, Suguitan ALJ, Cheng X, Subbarao K, Kemble G, Jin H. Glycosylation at 158N of the hemagglutinin protein and receptor binding specificity synergistically affect the antigenicity and immunogenicity of a live attenuated H5N1 A/Vietnam/1203/2004 vaccine virus in ferrets. J Virol. 2010; 84:6570–6577. [PubMed: 20427525]
31. Su Y, Yang HY, Zhang BJ, Jia HL, Tien P. Analysis of a point mutation in H5N1 avian influenza virus hemagglutinin in relation to virus entry into live mammalian cells. Arch Virol. 2008; 153:2253–2261. [PubMed: 19020946]
32. Lindsay LL, Kelly TR, Plancarte M, Schobel S, Lin X, Dugan VG, Wentworth DE, Boyce WM. Avian influenza: mixed infections and missing viruses. Viruses. 2013; 5:1964–1977. [PubMed: 23921843]
33. Mertens E, Dugan VG, Stockwell TB, Lindsay LL, Plancarte M, Boyce WM. Evaluation of phenotypic markers in full genome sequences of avian influenza isolates from California. Comp Immunol Microbiol Infect Dis. 2013; 36:521–536. [PubMed: 23891310]
34. Vandamme AM, Witvrouw M, Pannecouque C, Balzarini J, Van Laethem K, Schmit JC, Desmyter J, De Clercq E. Evaluating Clinical Isolates for Their Phenotypic and Genotypic Resistance Against Anti-HIV Drugs. Methods Mol Med. 2000; 24:223–258. [PubMed: 21331913]
35. Hara S, Takemori Y, Yamaguchi M, Nakamura M, Ohkura Y. Determination of alpha-keto acids in serum and urine by high-performance liquid chromatography with fluorescence detection. J Chromatogr. 1985; 344:33–39. [PubMed: 4086555]

Highlights

- Influenza A viruses utilize sialylated host glycans for attachment and infection
- A novel 3D glycan bead array enables detection and analysis of low abundance virus
- Virus glycan-binding specificity can be analyzed directly in primary samples
- The glycan-binding profile reflects the actual tropism of virus in nature

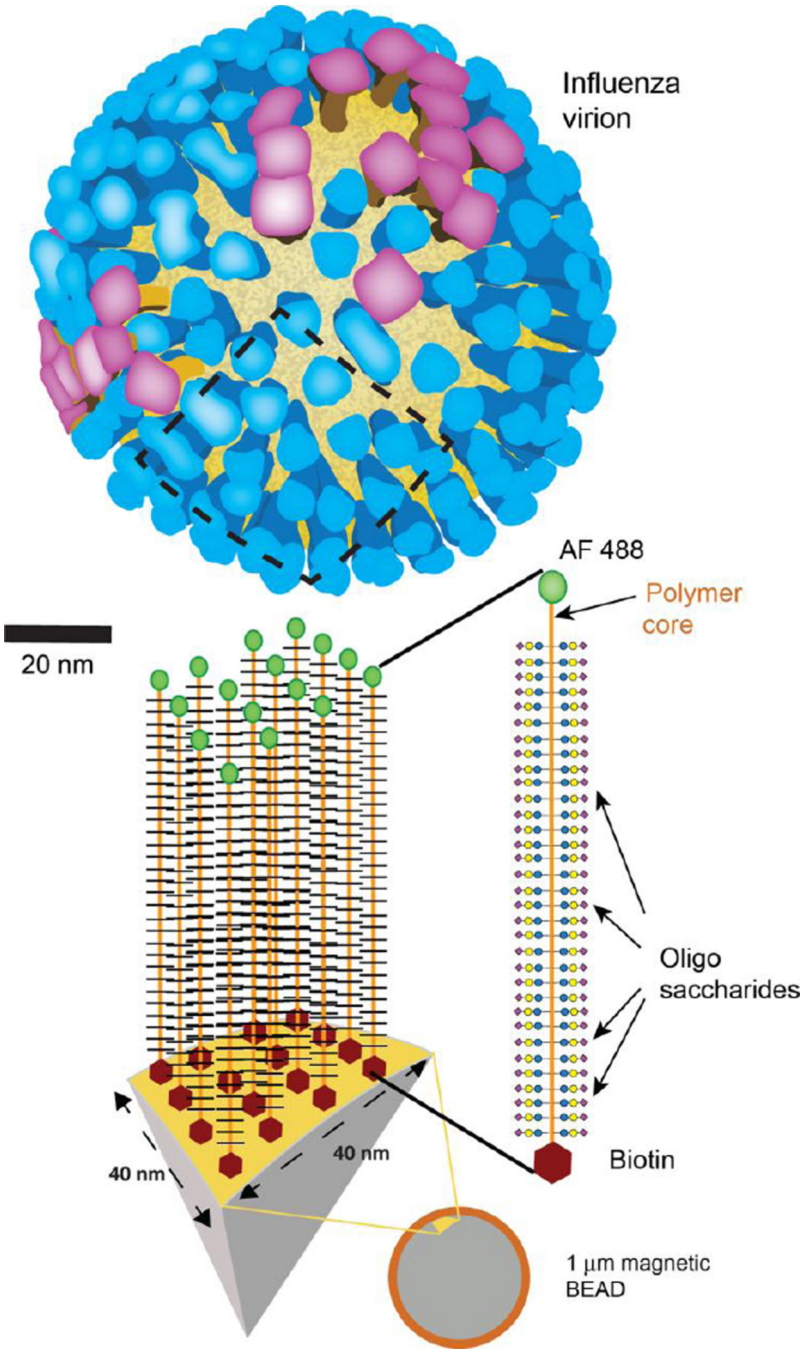

Figure 1.

Schematic representation of the 3D mucin mimetic bead array. Mucin mimetic glycopolymers are labeled with a single Alexa Fluor 488 (AF 488) fluorophore and a single biotin at the terminal ends. The glycopolymers are conjugated to streptavidin-coated magnetic bead at an average density of 27-molecules/1600 nm^2. Note that the density of HA spikes (blue) is approximately 13-molecules/1600 nm^2 and NA spikes (pink) cluster on the viral envelope (17).

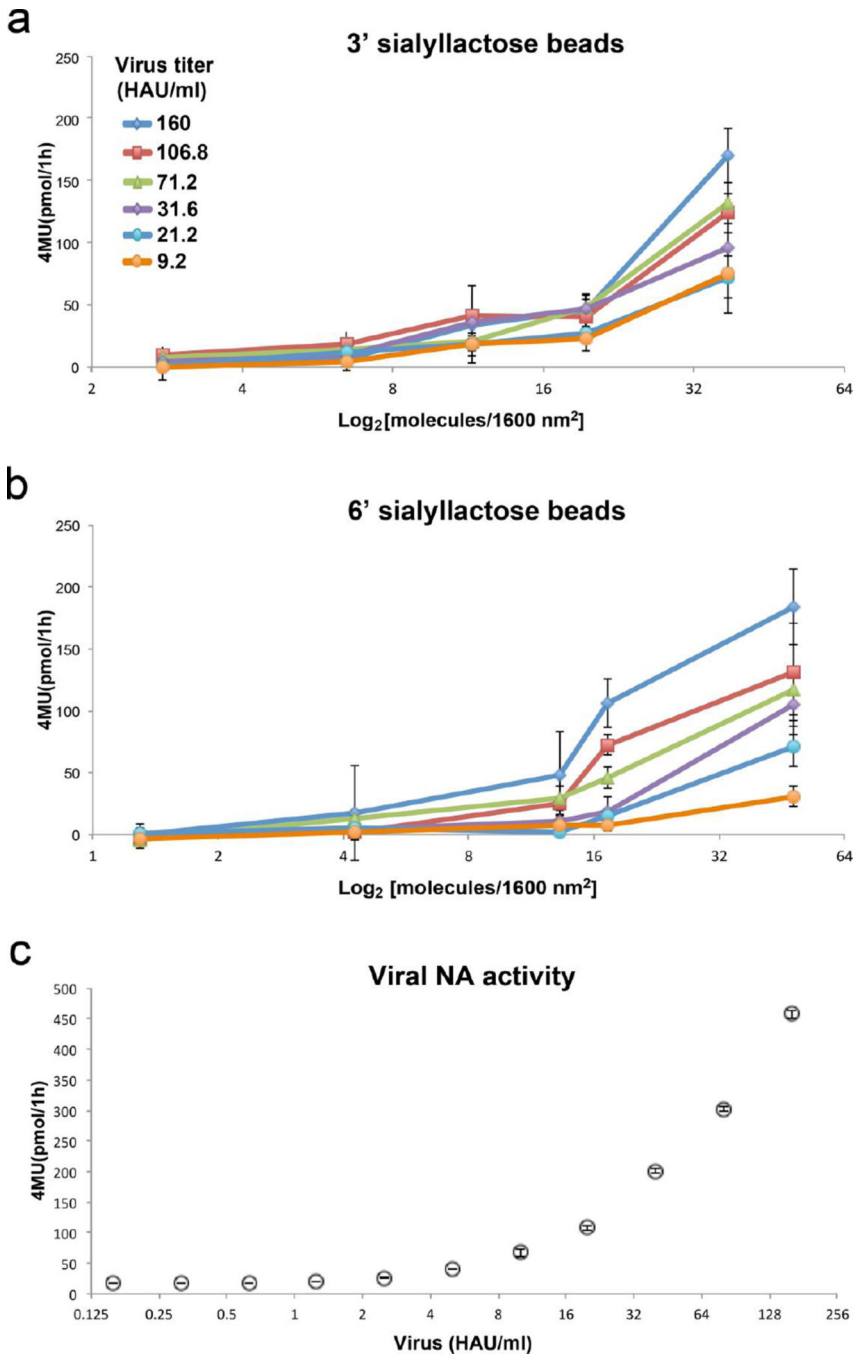

Figure 2.

Density dependent detection of A/PR/8/34(H1N1) binding to mucin mimetic beads. (**a**) 3'-sialyllactose and (**b**) 6'-sialylalactose mucin mimetic polymers were conjugated to magnetic beads at varying densities. The polymers density was calculated post conjugation as explained in supplementary Fig. 1. The binding of A/PR/8/34(H1N1) at 9.2–160 HAU/ml was tested on the array. To control for non-specific binding of virus to the beads, binding to lactose polymer conjugated beads at respective density was subtracted from the results. (**c**)

The NA activity of A/PR/8/34(H1N1) at 9.2–160 HAU/ml was quantified using the reporter molecule 4MU-NANA.

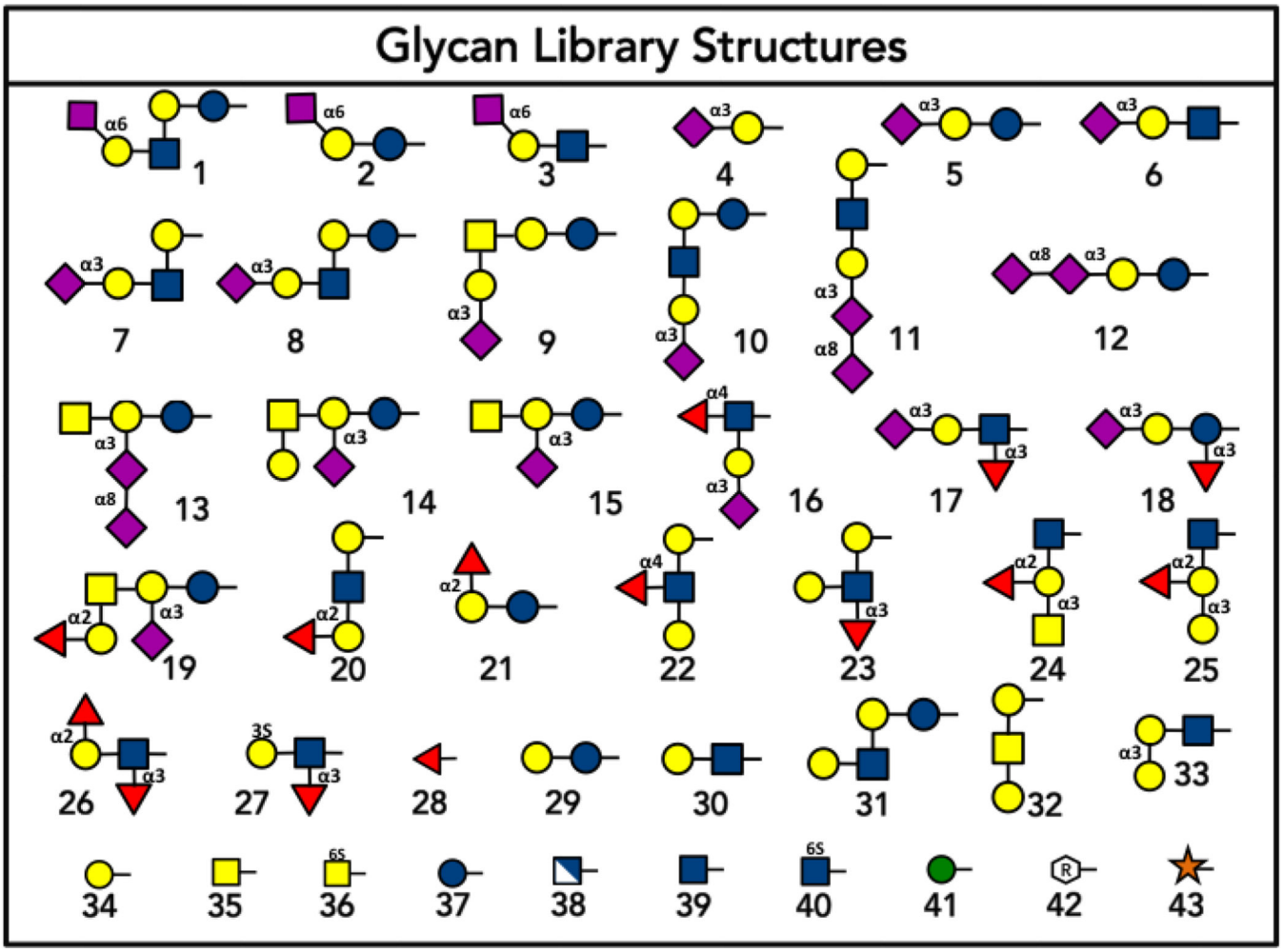

Figure 3.

Glycan library structures.

The numbering below the structures corresponds to the list of glycoconjugates in supplementary Table 1. In the diagram, horizontal glycosidic bonds represent β (1,4) linkages, while vertical bonds represent β (1,3) linkages, until otherwise indicated.

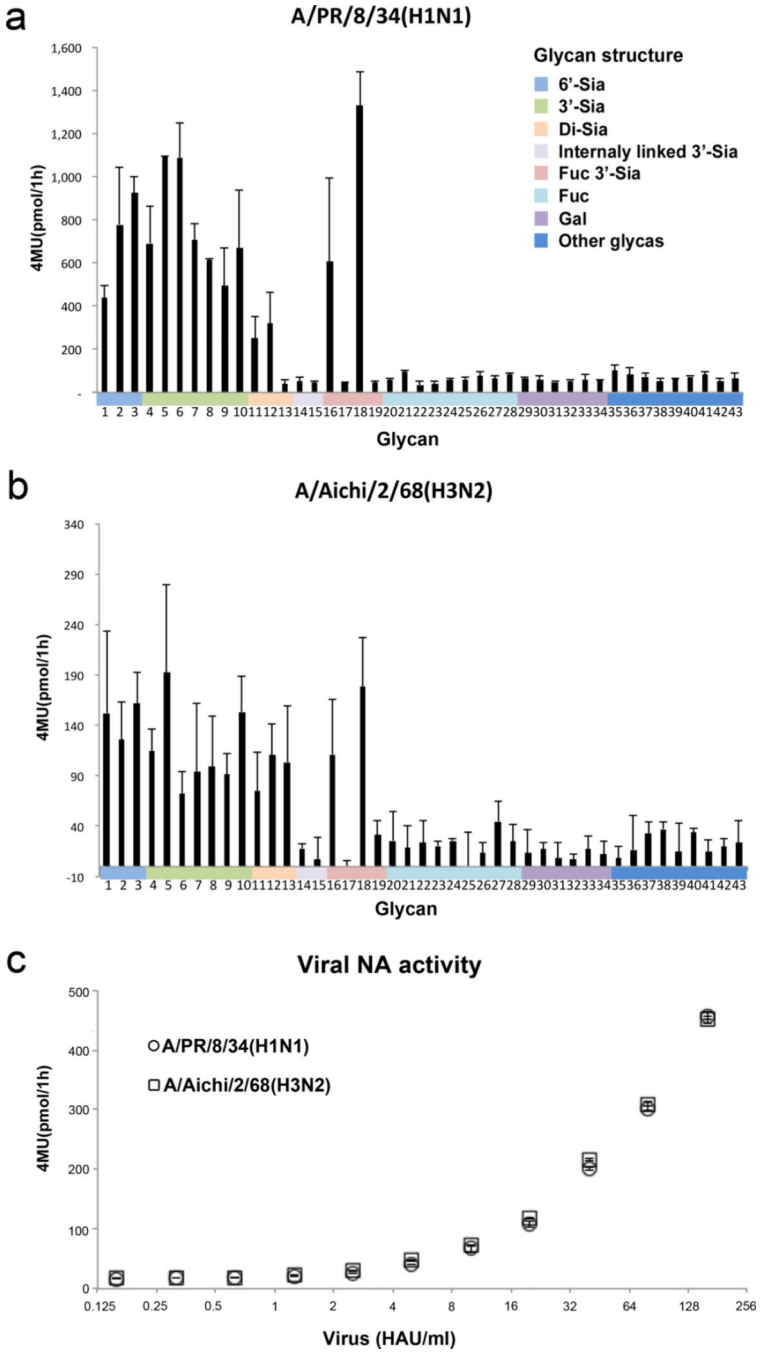

Figure 4.

Validation of the 3D mucin mimetic bead array. (**a**) The binding of A/PR/8/34(H1N1) and (**b**) A/Aichi/2/68(H3N2) at 64 HAU/ml was tested on an array of beads conjugated to a library of 43 mucin mimetic polymers. Error bar = s.d., n=3. (**c**) The NA activity of A/PR/8/34(H1N1) (circles) and A/Aichi/2/68(H3N2) (squares) at 9.2–160 HAU/ml was quantified using the reporter molecule 4MU-NANA.

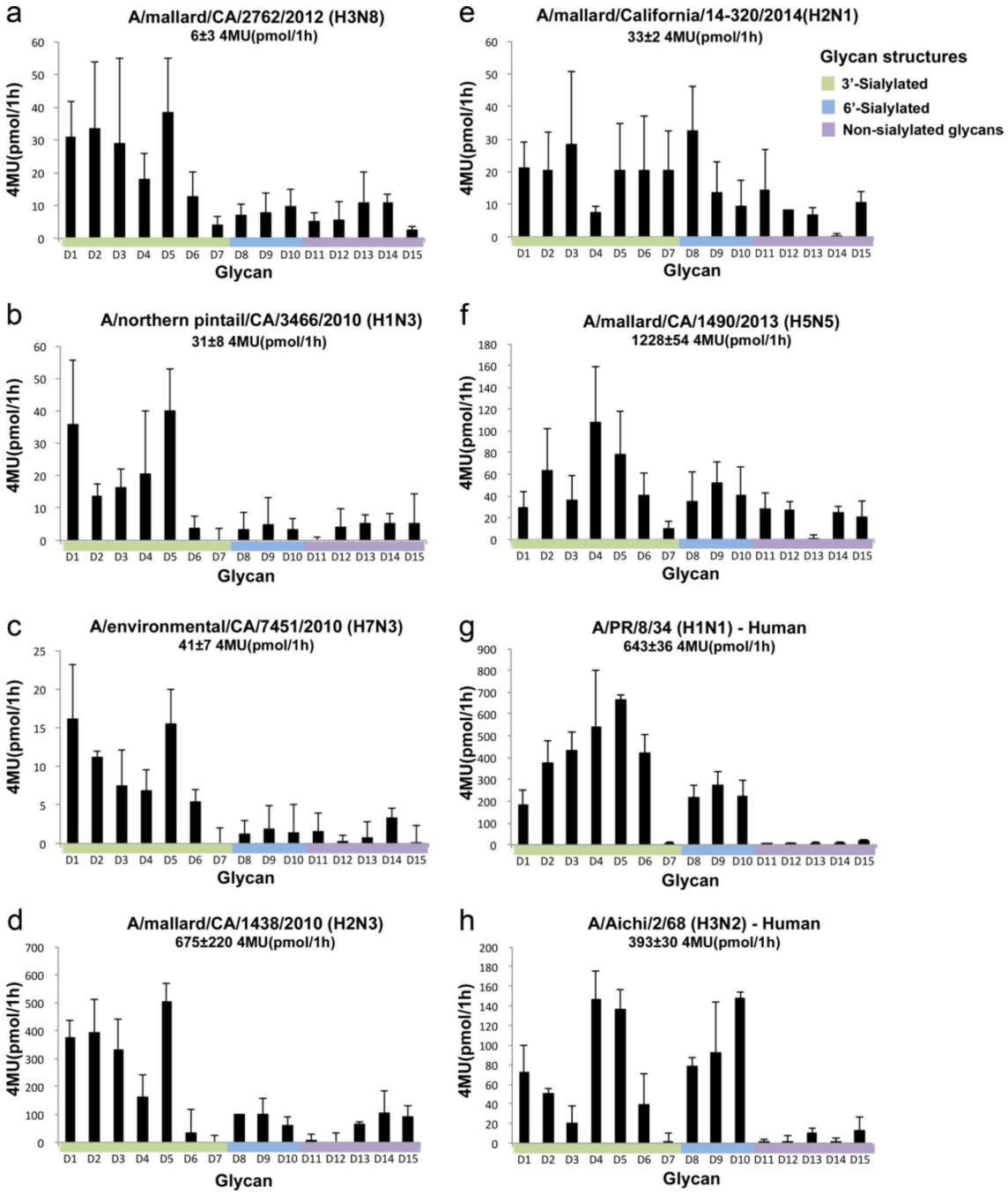

Figure 5.

Detection of avian IAV binding to the bead array. The binding of (**a–f**) six avian IAV and (**g–h**) two human IAV was tested on portion of the array containing pairs of 3'- and 6'-sialoglycoconjugates (detailed list in supplementary Table 3). NA activity of viral stock is noted at the title of each graph. (**a–d**) Expected binding to α2-3 linked sialic acids was observed for four of the subtypes. (**e–f**) A/mallard/California/14-320/2014(H2N1) and A/mallard/CA/1490/2013 (H5N5) bound sialoglycoconjugates in both α2-3 and α2-6 linkage. Error bar = s.d., n=3

a

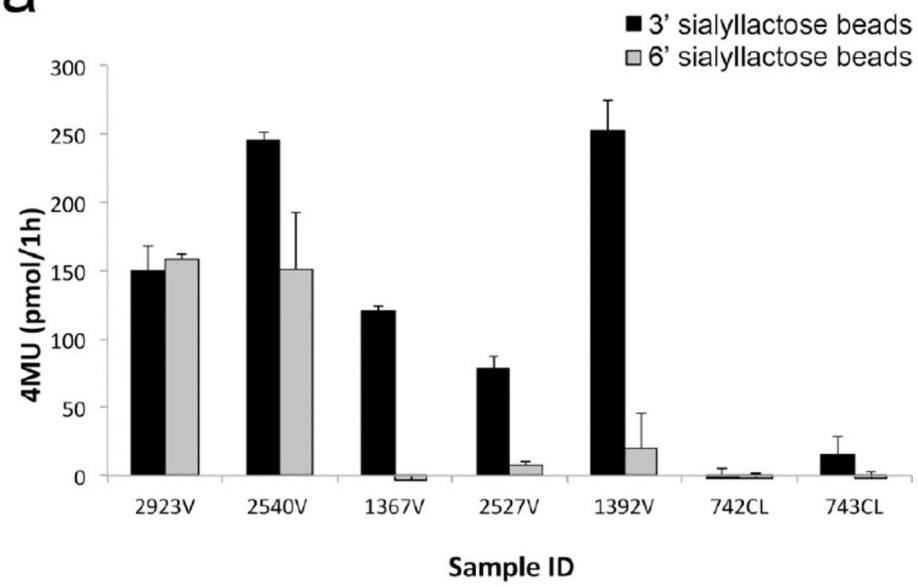

b

Sample ID	3' sialyllactose	6' sialyllactose	lactose
2923V	39.2740	37.6478	ND
2540V	40.7983	38.0560	ND
1367V	38.3498	39.5681	ND
2527V	39.2278	ND	ND
742CL	ND	ND	ND

c

Sample ID	JCVI Subtype	NA activity	HA activity
2923V	H3N8	176.9	ND
2540V	H3N8	566.7	160
1367V	mixed H4,H5 N5,N6	622.6	160
2527V	H5N1	724.4	ND
1392V	H5N5	967.4	NT
742CL	negative	5.5	ND
743CL	negative	1,500.2	ND

Figure 6.

Analysis of primary samples on mucin mimetic beads. (**a–b**) Cloacal swab samples from mallard ducks were directly applied to 3'-sialylalactose (black) and 6'-sialylalactose (gray) mucin mimetic beads. To control for non-specific binding to the beads, binding to lactose polymer conjugated beads was subtracted from the results. Bead bound virus was detected by quantifying NA activity (**a**) or by RT-PCR (**b**). Error bar = s.d., n=3. (**c**) The samples were analyzed at J. Craig Venter Institute to determine IAV subtype. The NA activity (pmol 4MU/1h) of each sample was quantified prior to bead capture using the 4MU-Neu5Ac

method, and HA activity (HAU/ml) was determined for turkey erythrocytes agglutination. ND= not detected, NT = not tested.